

# Land Surface Temperature Retrieval From GF5-01A Based on Split- Window Algorithm

Yu Liu <sup>1</sup>, YongXin Wang <sup>2,\*</sup>, GuangHui Wang <sup>1</sup>

<sup>1</sup> Land Satellite Remote Sensing Application Center, MNR, Beijing 100048, China-867532660@qq.com

<sup>2</sup> Beijing SatImage Information Technology Co. Ltd., Beijing, 100048, China-19376027@qq.com

**Keywords:** GF5-01A, Thermal Infrared, Split-Window Algorithm, LST

## Abstract

Land Surface temperature (LST) is a core parameter in the energy exchange between the surface and the atmosphere, and the use of thermal infrared remote sensing can realize the wide-range, fast, and accurate acquisition of surface temperature. GF5-01A is an important part and the final satellite of the major special project on high-resolution Earth observation system which is equipped with a wide-area thermal infrared imager with a resolution of 100 meters and a width of 1,500 kilometers. In this paper, based on the GF5-01A WTI spectral response function, combined with the TIGR2000 atmospheric profiles data and the ASTER spectral library, the data simulation was carried out by using the atmospheric radiative transfer model MODTRAN 5.2, and then constructed the split-window algorithm. Then, the method proposed in this paper was validated and evaluated using Landsat 8/9 temperature products and measured surface temperature data from SURFRAD sites acquired on the same day. The results show that the RMSE between the GF5-01A retrieved LST and the Landsat8/9 retrieved LST is between 1.27-2.24K, and the Bias is between -2.08-1.12K. The RMSE is between 0.68-2.64K and the bias is between -0.68-1.49K compared to the measured surface temperature. The split-window algorithm of GF5-01A proposed in this paper can meet the requirements of thermal infrared remote sensing monitoring and has enormous potential and value.

## 1. Introduction

LST is one of the key parameter in the physics of land-surface processes on regional and global scales (Sobrino et al., 2016). LST integrates surface-atmosphere interactions and energy exchanges between the atmosphere and land. LST can provide spatiotemporal information on the balance of surface energy, and has been widely applied in research fields such as numerical forecasting, global circulation models, regional climate models, (Li et al., 2016). According to the 2013 climate change report of the United Nations Intergovernmental Panel on Climate Change, the average temperature of the Earth's surface per decade has been warming steadily over the past three decades. Earth's climate change has become a major trend of climate change in the 21st century, which will lead to sea level rise and an increase in extreme weather, thus affecting the global ecosystem. Therefore, the acquisition and monitoring of surface temperature has been widely concerned by scholars from all over the world, and how to quickly and accurately acquire surface temperature has become a research hotspot in today's climate, ecological and environmental issues. The traditional way of acquiring LST not only consumes a lot of manpower and material resources, but also fails to meet the monitoring of temperature changes on a regional or even global scale. However, with the progress of science and technology, the quality and resolution of satellite remote sensing images have been improved by leaps and bounds, providing a reliable method for studying surface temperature on a regional or global scale and spatial and temporal variations in regions with long time series (Dash P et al., 2002). LST can be quickly and accurately obtained through thermal infrared remote sensing.

The GF5-01A is a Chinese civilian remote sensing satellites, part of a major project of the China High-definition Earth Observation System, which was successfully launched on December 9, 2022,

including a 1500 km swath width thermal infrared imager(WTI), a 2.5 nm spectral-resolution Visible-shortwave Infrared Advanced Hyperspectral Imager (AHSI), and a environmental trace gases monitoring instrument for atmospheric trace gasses (EMI). The satellite is based on the SAST1000. GF-501A is mainly used in environmental pollution monitoring, environmental quality supervision, atmospheric composition monitoring, natural resources investigation, climate change research, etc. WTI is the first thermal infrared detector in the world that adopts the thermal infrared detection mode with a width of 1,500 kilometers and a spatial resolution of 100 meters, and has the capability of all-day imaging during daytime and night time. WTI has 4 bands with spectral range 8.01 $\mu$ m~8.39 $\mu$ m, 8.42 $\mu$ m ~8.83 $\mu$ m, 10.3 $\mu$ m ~11.3 $\mu$ m, 11.5 $\mu$ m~12.5 $\mu$ m. The spectral response function is shown as Figure 1. Compared with the Landsat8/9 TIRS which has the same spatial resolution, the observation width has been increased by a factor of 7, and the number of thermal infrared observation channels (4) has been increased by a factor of 1, so that global-scale high-precision surface temperature information can be obtained inversely.

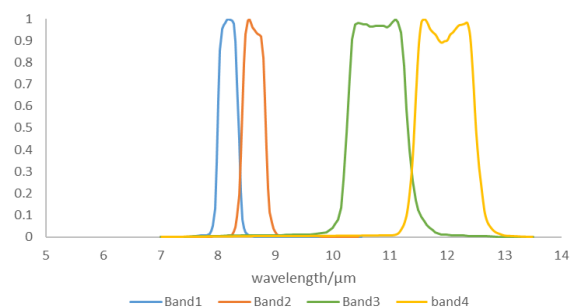


Figure 1. Spectral response function

\* Corresponding author

Since the last century, scholars at home and abroad have conducted a large number of scientific studies using thermal infrared data, proposed a variety of surface temperature inversion algorithms based on the characteristics of different sensors, and then improved the algorithms on the basis of this, to reduce the interference caused by the atmospheric and surface emissivity, and to enhance the inversion accuracy. The methods for surface temperature can be roughly divided into single-channel algorithms, multi-channel algorithms, and multi-angle algorithms. The split-window algorithm is a type of multi-channel algorithm, which has been widely used due to its advantages of fewer input parameters, simple algorithm, and low sensitivity to atmospheric parameters. The objective of this study is to develop a split-window algorithm to retrieve LST from GF5-01A.

## 2. Study Area

### 2.1 Cross-validation test area

In order to verify the availability of the GF5-01A split-window algorithm, this study selected 5 areas in Jiangsu (Taihu Lake, Hongze Lake), Shandong(Qingdao), Qinghai(Qinghai Lake), Inner Mongolia(The Badain Jaran Desert) in China as cross validation test areas according to the acquisition of synchronous remote sensing image data and land cover types. Taihu Lake, Hongze Lake, Qinghai Lake were selected as the water validation area. The Badain Jaran Desert was selected as the sand validation area. Qingdao was selected as the vegetation validation area. The cross-validation region is shown in Figure 2.

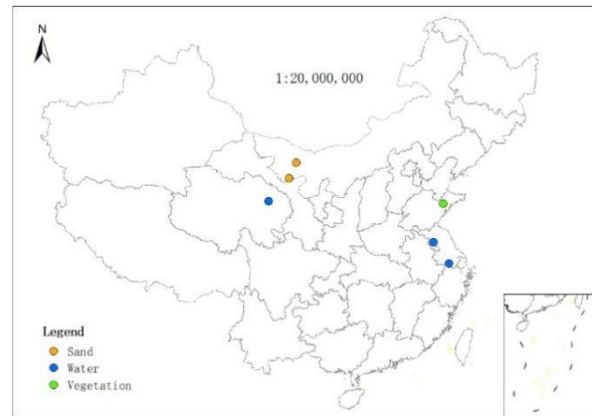


Figure 2. Cross-validation test area

### 2.2 SURFRAD

A surface radiation budget observing network (SURFRAD) has been established for the United States in 1993 to support climate research with accurate, continuous, long-term measurements of the surface radiation budget. Currently seven SURFRAD stations are operating in climatologically diverse regions: Montana, Colorado, Illinois, Mississippi, Pennsylvania, Nevada and South Dakota as shown in Table 1. The primary measurements are the downwelling and upwelling components of broadband solar and thermal infrared irradiance(Augustine et al.,2020). The main parameters of the site are measured every three minutes before 2019, and the measurement of once every minute after 2019.

Code	Name	Latitude	Longitude	Land Cover Type	Elevation	Installed
BND	Bondville, Illinois	40.05°N	88.37°W	Croplands	230m	April 1994
TBL	Table Mountain, Boulder, Colorado	40.13°N	105.24°W	Grassland	1689m	July 1995
FPK	Fort Peck, Montana	48.31°N	105.10°W	Grassland	634m	November 1994
SXF	Sioux Falls, South Dakota	43.73°N	96.62°W	Cropland	473m	June 2003
PSU	Penn. State Univ., Pennsylvania	40.72°N	77.93°W	Cropland/natural vegetation mosaic	376m	June 1998
GWN	Goodwin Creek, Mississippi	34.25°N	89.87°W	Woody Savannas	98m	December 1994
DRA	Desert Rock, Nevada	36.63°N	116.02°W	Open shrublands	1007m	March 1998

Table 1. SURFRAD Network



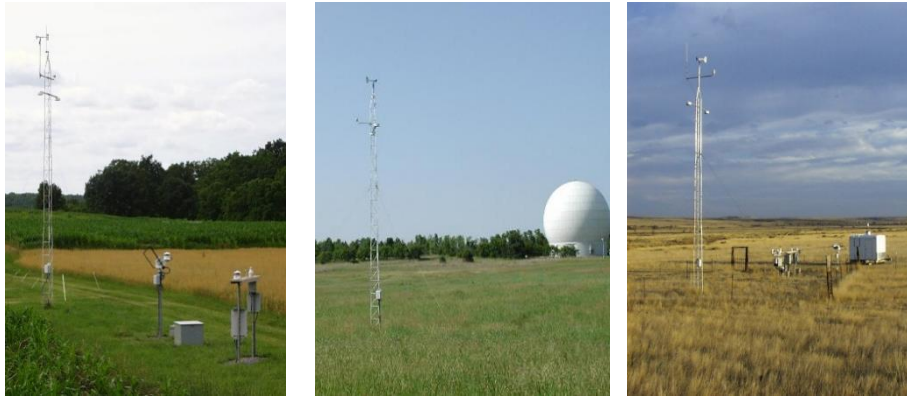


Figure 3. Observation instruments and surrounding environment in SURFRAD study sites  
 (Image Source: NOAA Earth System Research Laboratory)

### 3. Method

#### 3.1 Split-Window Algorithm Principle

Assuming a cloud-free atmosphere under local thermodynamic equilibrium, radiance received by satellite sensors can be described using the Radiative Transfer Equation (Li, et al.,2016).

$$L_{\lambda}^{sensor} = [\varepsilon_{\lambda}B(T_s) + (1 - \varepsilon_{\lambda})L_{\lambda}^{atm\downarrow}] \tau_{\lambda} + L_{\lambda}^{atm\uparrow} \quad (1)$$

$$T_s = \frac{K_2}{\ln\left(\frac{K_1}{B(T_s)} + 1\right)} \quad (2)$$

$$K_1 = \frac{hc^2}{\lambda^5} \quad (3)$$

$$K_2 = \frac{hc}{k\lambda} \quad (4)$$

Where  $L_{\lambda}^{sensor}$  is the top of the atmosphere(TOA) radiance,  $\varepsilon_{\lambda}$  is the surface emissivity,  $T_s$  is the LST,  $L_{\lambda}^{atm\downarrow}$  is the atmospheric downwelling radiances,  $L_{\lambda}^{atm\uparrow}$  is the atmospheric upwelling radiances,  $\tau_{\lambda}$  is the atmospheric transmittance,  $B$  is the Planck function,  $k$  is the Boltzmann's constant,  $\lambda$  is the central wavelength,  $c$  is the constant.

The split-window algorithm takes advantage of the difference in atmospheric absorption between two adjacent thermal infrared channels centered at about 11 and 12  $\mu\text{m}$ , and performs nonlinear analysis of the radiation transfer equation based on brightness temperatures (Sobrino et al.,1994; Sun D et al., 2003,2005,2007) to remove the influence of the atmosphere (McMillin et al.,1975), and then the surface temperature is inverted.

$$T_s = a_0 + a_1T_i + a_2(T_i - T_j) + a_3(T_i - T_j)^2 \quad (5)$$

where  $T_i$  and  $T_j$  are the TOA brightness temperatures measured in channels  $i$  ( $\sim 11.0 \mu\text{m}$ ) and  $j$  ( $\sim 12.0 \mu\text{m}$ ).  $a_i$  ( $i=0,1,2,3$ ) are the algorithm coefficients derived in the following simulated dataset.

#### 3.2 Algorithm Development for GF5-01A

In order to fit  $a_i$ , we used TIGR2000 atmospheric profiles for data simulation and constructed the dataset. One of the assumed conditions for the transfer of thermal infrared radiation is clear skies and no clouds. So the profiles with a relative humidity greater than 90% or two consecutive layers of relative humidity greater than 85% are discarded. As a result, a total of 946 atmospheric profile data were used for this simulation. Observation zenith angle setting range from  $0^\circ$  to  $20^\circ$  in a  $10^\circ$  step. The LST range from  $T_0 - 10 \text{ K}$  to  $T_0 + 25 \text{ K}$  in a  $5 \text{ K}$  step

where the  $T_0$  is atmospheric bottom temperature. In addition, the surface emissivity is obtained by convolving the spectral response function of the thermal infrared channel with the spectral curves from 101 spectrogram libraries which are comes from the ASTER Spectral Library. According to the simulation dataset,  $L_{\lambda}^{atm\downarrow}$ ,  $L_{\lambda}^{atm\uparrow}$ ,  $\tau_{\lambda}$  in Equation(1) are calculated by the MODTRAN 5.2 atmospheric transmittance/radiance code. Finally, according to Equation (1) and Equation (5), the brightness temperatures  $T_i$  and  $T_j$  are obtained.  $a_i$  is calculated using the least squares method, and the results are shown in the Table2. LST from GF5-01A inversion was shown in Figure 4.

$a_0$	$a_1$	$a_2$	$a_3$
-11.8806	1.05547	-0.0398976	0.453618

Table 2. The results of  $a_i$

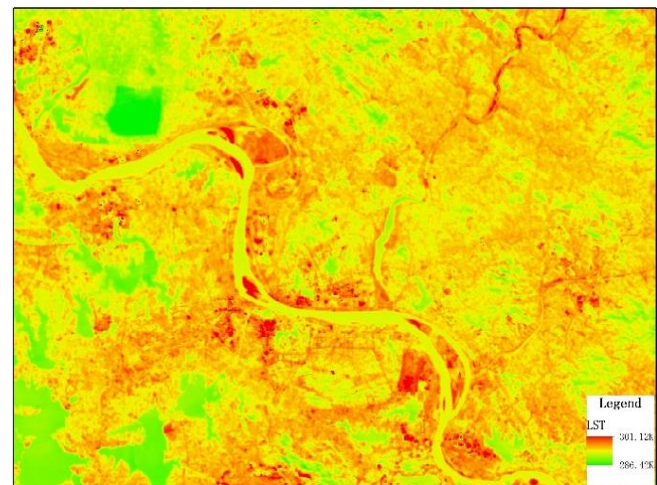


Figure 4. LST from GF5-01A inversion

## 4. Result and Analysis

### 4.1 Evaluation indicators

Root mean square error (RMSE) and Bias were selected to analyze and evaluate the accuracy of the GF5-01A split-window algorithm in this paper. RMSE evaluates the closeness between surface temperature inversion and actual land surface temperature. Bias evaluates the average difference between the surface temperature inversion and the actual surface temperature, reflecting the systematic bias of the inversion results.

$$RMSE = \sqrt{\frac{\sum(T_{inv} - T_{ref})^2}{n - 1}} \quad (6)$$

$$Bias = \frac{\sum T_{inv} - T_{ref}}{n} \quad (7)$$

Where  $T_{inv}$  is the LST inverted from thermal infrared remote sensing image,  $T_{ref}$  is the reference or measured LST, and  $n$  is the number of pixels.

#### 4.2 Cross-validation method

Cross-validation is the comparison of surface temperature inversion results with other surface temperature products that have been validated with high accuracy (Jiménez et al., 2012; Trigo et al., 2008). Under different surface cover conditions, such as water bodies, sand, vegetation, etc., manually and randomly selected feature points, such as Figure 5, were statistically analyzed and compared with Landsat 8/9 temperature products obtained on the same day which has the same spatial resolution and similar spectral response functions to verify the accuracy of surface temperature inversion using the split-window algorithm. Firstly, register Landsat temperature products with GF5-01A to reduce errors caused by geometric factors. Then, select relatively uniform surface cover such as water, vegetation, and sands, randomly select several validation points, and conduct analysis and evaluation. The results were shown as Figure 6 and Figure 7.

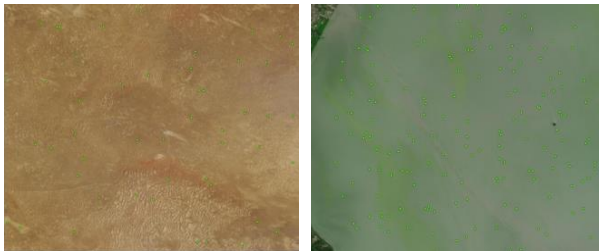


Figure 5. The distribution of verification point

As a whole, the RMSE of the difference between the GF5-01A retrieved LST and the Landsat8/9 retrieved LST is 1.72, and the Bias is 0.41. The inversion accuracy of water bodies is the highest. The relative accuracy of water is the highest, which the RMSE is 1.27 and the Bias is 1.12. The relative accuracy of sands is the worst, which the RMSE is 2.24 and the Bias is -2.08, because of the surface of the sands is uneven and affected by radiation directionality. The preliminary results indicate that the split-window algorithm of GF5-01A can meet the application needs and has enormous potential and value.

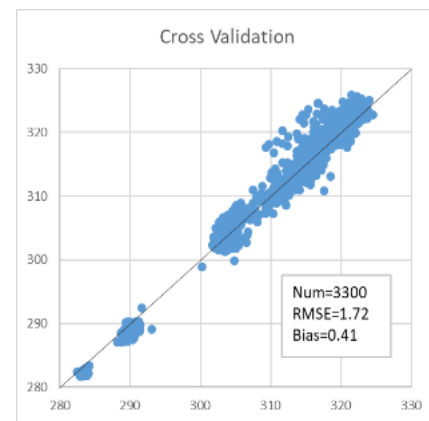


Figure 6. The results of validation

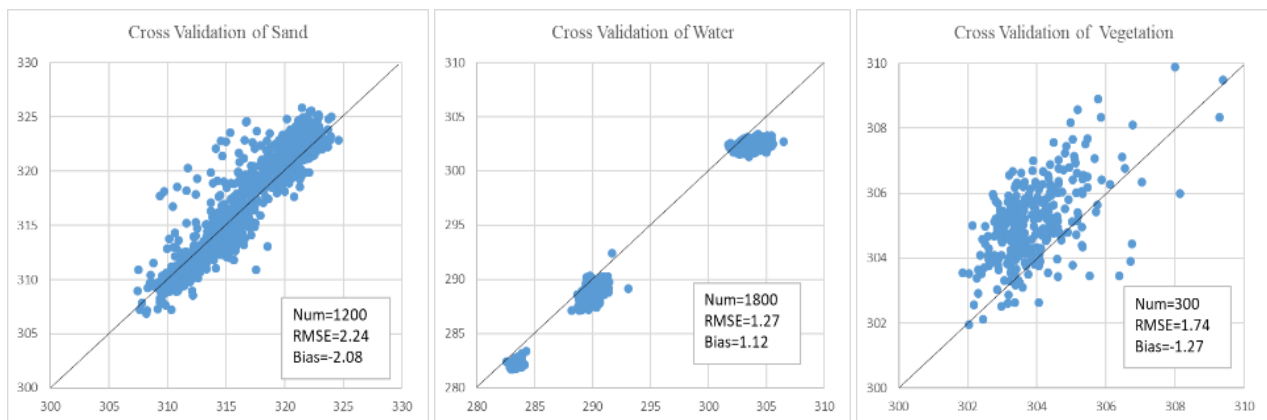


Figure 7. The results of validation

#### 4.3 Temperature-based method

In order to evaluate the availability of the GF5-01A split-window algorithm in this paper, the inverted surface temperatures of the clear-sky GF5-01A WTI data since March 2023 were used to analyze the inverted surface temperatures with the measured by SURFRAD sites.

In-situ longwave radiation measurements by the SURFRAD network were converted to LST values based on Stefan-Boltzmann law as follows (Li et al., 2014):

$$T_s = \left( \frac{L_{\lambda}^{atm\uparrow} - (1 - \varepsilon_{bb})L_{\lambda}^{atm\downarrow}}{\sigma \varepsilon_{bb}} \right)^{\frac{1}{4}} \quad (8)$$

Where  $T_s$  is the LST,  $L_{\lambda}^{atm\uparrow}$  is the measured surface upwelling longwave radiation,  $\epsilon_{bb}$  is the surface broadband emissivity,  $\sigma$  is the Stefan-Boltzmann constant ( $5.67 \times 10^{-8} \text{Wm}^{-2}\text{K}^{-4}$ ), and  $L_{\lambda}^{atm\downarrow}$  is the measured surface downwelling longwave radiation. The  $\epsilon_{bb}$  was calculated from the Aster GED product using the following linear equation (Duan et al.,2019; Cheng et al.,2012; Cheng et al.,2012):

$$\epsilon_{bb} = 0.197 + 0.025\epsilon_{10} + 0.057\epsilon_{11} + 0.237\epsilon_{12} + 0.333\epsilon_{13} + 0.146\epsilon_{14} \quad (9)$$

Where The  $\epsilon_{10}$ – $\epsilon_{14}$  are the narrow-band surface emissivities of the ASTER bands 10–14, respectively. The surface broadband emissivities are 0.968, 0.972, 0.967, 0.973, 0.971, 0.970, and 0.970 for BND, TBL, DRA, FPK, GWN, PSU, and SXF, respectively.

A total of 9 pairs of data were collected for this validation, covering 4 sites which were DRA, BND, TBL & PSU. The results are shown in Table 3. The scatterplot between the measured temperature and the retrieved temperature is shown in Figure 8.

Sites	Numbers	RMSE	Bias
DRA	4	2.64	0.72
BND	2	1.74	1.49
TBL	2	1.68	0.45
PSU	1	0.68	-0.68
Total	10	2.11	0.68

Table 3. RMSE and Bias between LST retrieved by GF5-01A and measured by SURFRAD sites

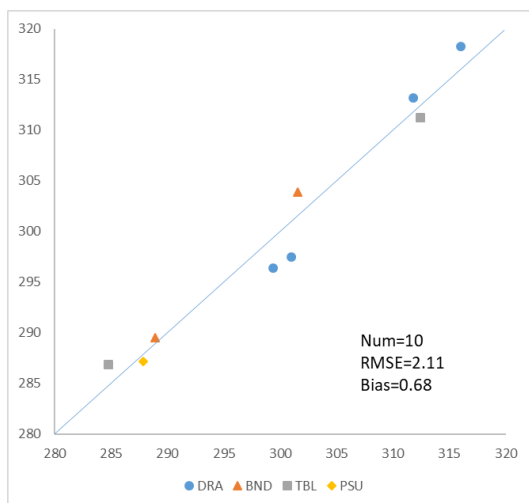


Figure 8. Compared with the measured temperature and retrieved temperature

In the process of validating the results, this paper refers to the method of Sobrino et al. for rejecting outliers (Sobrino et al.,2019). Overall, Compared with the measured temperature and retrieved temperature, the RMSE for each site ranged from 0.68-2.56 K, and total RMSE is 2.11 K. Validation results for BND, TBL, and PSU sites RMSE values are higher than DRA. This may be related to the site subsurface, where the DRA site is collocated with the

Desert Rock, the surface is rough and more affected by the directionality of the radiation. Bias values are less than 1K at all sites except the BND. From another point of view, the validation results of surface temperature for the 3 sets of nighttime data are better than those of the daytime data. This may be related to the poor isothermal properties of heterogeneous surface pixels during the daytime, and the large temperature differences in the light and shadow areas within the pixels due to the relationship between solar irradiation and the angle of remote sensing observations (Coll et al.,2019; Li et al.,2014; Guillevic et al.,2014; Hale et al.,2011).

## 5. Conclusions

a key physical parameter for various studies, including hydrology, climatology, the environment, and ecology (Duan et al.,2008; Anderson et al.,2008; Sobrino et al.,2014). In this study, we proposed a split-window algorithm for LST retrieval from GF5-01A thermal infrared channel. Completed relative accuracy verification with Landsat surface temperature products on water, vegetation and sands that the overall RMSE is 1.72 and Bias is 0.41. Meanwhile, comparisons were made with measured data from the SURFRAD sites, where the RMSE was 2.11K and the bias was 0.68K. The results show that the proposed algorithm can be used to retrieve LST. However, the evaluation of the accuracy of the split-window algorithm still needs to be carried out in depth due to the small amount of measured data. Furthermore, to better evaluate the accuracies of the method, more LST validation works need to be performed under various atmospheric conditions and land-cover types.

## References

- Anderson M C, Norman J M, Kustas W P, et al. A thermal-based remote sensing technique for routine map\*\* of land-surface carbon, water and energy fluxes from field to regional scales[J]. *Remote Sensing of Environment*, 2008, 112(12): 4227-4241.
- Augustine J A, DeLuisi J J, Long C N. SURFRAD—A national surface radiation budget network for atmospheric research[J]. *Bulletin of the American Meteorological Society*, 2000, 81(10): 2341-2358.
- Cheng Y L, Wu H, Li Z L and Qian Y G. 2021. Retrieval and validation of the land surface temperature from FY3D MERSI-II. *National Remote Sensing Bulletin*, 25(8):1792-1807.
- Dash P, Göttsche F M, Olesen F S, et al. Land surface temperature and emissivity estimation from passive sensor data: Theory and practice-current trends[J]. *International Journal of remote sensing*, 2002, 23(13): 2563-2594.
- Duan S B, Li Z L, Li H, et al. Validation of Collection 6 MODIS land surface temperature product using in situ measurements[J]. *Remote sensing of environment*, 2019, 225: 16-29.
- Guillevic P C, Biard J C, Hulley G C, et al. Validation of Land Surface Temperature products derived from the Visible Infrared Imaging Radiometer Suite (VIIRS) using ground-based and heritage satellite measurements[J]. *Remote Sensing of Environment*, 2014, 154: 19-37.
- Hale R C, Gallo K P, Tarpley D, et al. Characterization of variability at in situ locations for calibration/validation of satellite-derived land surface temperature data[J]. *Remote Sensing Letters*, 2011, 2(1): 41-50.

Hu T, Li H, Cao B, et al. Influence of emissivity angular variation on land surface temperature retrieved using the generalized split-window algorithm[J]. *International journal of applied earth observation and geoinformation*, 2019, 82: 101917.

Jiménez C, Prigent C, Catherinot J, et al. A comparison of ISCCP land surface temperature with other satellite and in situ observations[J]. *Journal of Geophysical Research: Atmospheres*, 2012, 117(D8).

Li S, Yu Y, Sun D, et al. Evaluation of 10 year AQUA/MODIS land surface temperature with SURFRAD observations[J]. *International Journal of Remote Sensing*, 2014, 35(3): 830-856.

Li Z L, Duan S B, Tang B H, et al. Review of methods for land surface temperature derived from thermal infrared remotely sensed data[J]. *Journal of remote sensing*, 2016, 20(5): 899-920.

McMillin L M. Estimation of sea surface temperatures from two infrared window measurements with different absorption [J]. *Journal of Geophysical Research*, 1975,80(36): 5113–5117.

Rozenstein O, Qin Z, Derimian Y, et al. Derivation of land surface temperature for Landsat-8 TIRS using a split window algorithm[J]. *Sensors*, 2014, 14(4): 5768-5780.

Sobrino J A, Jiménez-Muñoz J C, Soria G, et al. Synergistic use of MERIS and AATSR as a proxy for estimating Land Surface Temperature from Sentinel-3 data[J]. *Remote sensing of environment*, 2016, 179: 149-161.

Sobrino J A, Jiménez-Muñoz J C. Minimum configuration of thermal infrared bands for land surface temperature and emissivity estimation in the context of potential future missions[J]. *Remote sensing of environment*, 2014, 148: 158-167.

Sobrino J A, Li Z L, Stoll M P, et al. Improvements in the split-window technique for land surface temperature determination[J]. *IEEE Transactions on Geoscience and Remote Sensing*, 1994, 32(2): 243-253.

Sun D, Pinker R T. Estimation of land surface temperature from a Geostationary Operational Environmental Satellite (GOES - 8)[J]. *Journal of geophysical research: atmospheres*, 2003, 108(D11).

Sun D, Pinker R T. Implementation of GOES-based land surface temperature diurnal cycle to AVHRR[J]. *International Journal of Remote Sensing*, 2005, 26(18): 3975-3984.

Sun D, Pinker R T. Retrieval of surface temperature from the MSG - SEVIRI observations: Part I. Methodology[J]. *International Journal of Remote Sensing*, 2007, 28(23): 5255-5272.

Trigo I F, Monteiro I T, Olesen F, et al. An assessment of remotely sensed land surface temperature[J]. *Journal of Geophysical Research: Atmospheres*, 2008, 113(D17).

Zhu J S, Ren H Z, Ye X, et al. Ground validation of land surface temperature and surface emissivity from thermal infrared remote sensing data: A review[J]. *National Remote Sensing Bulletin*, 2021, 25(8): 1538-1566.